

# Scattering and Reactions of Halo Nuclei

— *A Theorist's Perspective* —

Ronald JOHNSON<sup>\*)</sup>

*Physics Department, University of Surrey, Guildford, Surrey GU2 7XH, UK*

(Received June 15, 2000)

In this talk I describe some theoretical techniques which have provided a useful insight into reactions involving light exotic systems.

## §1. Introduction

One of the most exciting scientific developments in recent years has been the advent of accelerated beams of radioactive nuclei with exotic combinations of neutron and proton numbers. The new techniques produce beams of nuclei which decay by the weak interaction but are stable against decay into their constituents. Nuclear reactions induced by beams incident on targets of ordinary stable nuclei are important sources of information about the structure of the exotic species. For example, experiments of this type led to the discovery of the important new class of nuclei known as halo nuclei.<sup>1)-3)</sup>

New experiments are extending our understanding of these novel systems, but the mechanism involved in reactions involving halos and other nuclei far from the valley of stability presents a special challenge to theorists. An important consideration is that exotic nuclei are often very weakly bound and easily broken up in the Coulomb and nuclear fields of the target nucleus. Halo nuclei are an extreme case with almost zero binding energy. As a consequence, theories which deal with excitations of the projectile are a prerequisite if reliable information on nuclear structure is to be deduced from reaction experiments. On the other hand, many of the relevant experiments, both current and planned, involve projectile energies which allow simplifying assumptions to be made which help to make the theory more transparent. I will present some of the insights obtained in this way together with illustrations from recent experiments and a discussion of the implication of the new theories for future experimental programmes.

## §2. One-neutron halo nuclei

Some key features of halo nuclei<sup>4)</sup> remind us of some familiar features of the deuteron. For present purposes we can ignore the small deuteron  $D$ -state and consider the deuteron to be a  $1S$  state in an attractive  $n$ - $p$  potential of depth about 30 MeV and range about 1 fm. The deuteron has a binding energy of  $\epsilon_d = 2.2$  MeV. Quantum mechanics tells us that in the classically forbidden region where the  $n$ - $p$

---

<sup>\*)</sup> E-mail address: R.Johnson@Surrey.ac.uk

separation  $r$  is bigger than 1 fm the space part of the deuteron's wavefunction will have the form

$$\phi_0 = N_d \frac{\exp(-\lambda_d r)}{r}, \quad r > 1 \text{ fm}, \quad (2.1)$$

where  $N_d$  is a normalisation constant. The constant  $\lambda_d$  is determined from the deuteron binding energy by  $\lambda_d = \sqrt{2\mu\epsilon_d/\hbar^2}$  where  $\mu$  is the reduced mass of the  $n$ - $p$  system. This is the functional form predicted by Yukawa for the interaction associated with the exchange of massive particles. Particle exchange also proceeds through classically forbidden regions and hence gives rise to the same functional dependence on distance.

The small deuteron binding energy results in the value  $1/\lambda_d = 4.2$  fm which is much larger than the range of the  $n$ - $p$  interaction and means that in the deuteron the neutron and proton spend a significant part of the time in the classically forbidden region. Indeed, for many purposes its a good approximation to approximate the deuteron wavefunction by the form Eq. (2.1) for *all* values of  $r$ .

The one-neutron halo nucleus  $^{11}\text{Be}$  can be described in a similar picture. It costs 0.503 MeV to remove a neutron from  $^{11}\text{Be}$  and leave  $^{10}\text{Be}$  in its ground state. The simplest version of the halo model describes the corresponding component of the  $^{11}\text{Be}$  wavefunction as a  $^{10}\text{Be}$  core and a neutron in an  $S$ -state. For  $n$ -core separations  $r$  bigger than the core radius the neutron wavefunction is

$$\phi_0 = N_{11} \frac{\exp(-\lambda_{11} r)}{r}, \quad (2.2)$$

where  $1/\lambda_{11} = 6.7$  fm as determined by the neutron separation energy.

The key point here is that  $1/\lambda_{11}$  is much bigger than the size of the core so that the classically forbidden region outside the core plays a very important role, just as in the case of the deuteron.

There are however some important differences between the  $d$  and  $^{11}\text{Be}$  cases. In the first place, unlike the deuteron,  $^{11}\text{Be}$  has a bound excited state with a separation energy of 0.18 MeV. Second the Pauli principle demands that the ground state of  $^{11}\text{Be}$  be a  $2S$  state with a node in the core region in contrast with the nodeless function which simple potential models give for the deuteron. This reflects the fact that underlying this 2-body picture of  $^{11}\text{Be}$  is a many fermion system.

The qualitative features associated with very weak binding suggests that an approach based on the 2-body picture might be a good starting point for studying the structure of  $^{11}\text{Be}$ , in contrast with mean field models which emphasise the identity of all nucleons. It is this possibility of an alternative good starting point for models of their structure that makes halo systems interesting from a theoretical point of view. For an excellent bibliography and a discussion of corrections to the basic few-body models see Ref. 5).

In this talk I will concentrate on one-neutron halos. Much of what I have to say is also relevant to multi-neutron halos such as the famous two-neutron halo  $^{11}\text{Li}$ .<sup>1),4)</sup>

### §3. Nuclear reaction theory

Nuclear reactions play a crucial role in the study of nuclei and halo nuclei are no exception. Well developed theories of nuclear reactions already exist.<sup>10)</sup> The interesting questions for theory are whether these theories will work for reactions involving halo nuclei, and if not, how should they be modified.

The weak binding of halo nuclei makes a positive answer to the first question unlikely. The weak binding of the neutron to  $^{11}\text{Be}$  means that the halo degree of freedom is easily excited by the nuclear and Coulomb fields of target nucleus. The weak binding also means that even a small transfer of momentum from the relative motion of the 2 nuclei will excite the halo nucleus into the continuum of unbound states from which fragments may propagate to large distances. It is very difficult to treat such configurations realistically especially when one or more of the fragments is charged.

#### 3.1. Coupled channels formulations

It is natural to base the reaction theory for halo systems on few-body models. Here I emphasise approaches which treat only the halo degrees of freedom explicitly, the other nuclear sub-systems being parameterised in terms of effective 2-body interactions.

As a concrete example we consider a 3-body model of reactions induced by a  $^{11}\text{Be}$  projectile on a  $^{12}\text{C}$  target. The 3 bodies involved are the  $^{10}\text{Be}$  core and the halo neutron which make up our model of the projectile and the target. This system has been studied at GANIL at beam energies of 50 MeV/A. A suitable set of co-ordinates to describe the system is shown in Fig. 1. The Hamiltonian in the over-all centre of mass system is assumed to be

$$H = T_R + H_{nC} + V_{nT}(\vec{r}_{nT}) + V_{CT}(\vec{r}_{CT}), \quad (3.1)$$

where  $T_R$  is the kinetic energy of the 3-bodies and  $H_{nC}$  is the Hamiltonian for the  $n$ - $C$  relative motion.

$$T_R = -\frac{\hbar^2}{2\mu_{PT}} \nabla_R^2, \quad H_{nC} = -\frac{\hbar^2}{2\mu_{nC}} \nabla_r^2 + V_{nC}(\vec{r}), \quad (3.2)$$

where  $\mu_{PT}$  and  $\mu_{nC}$  are reduced masses. The 2-body potentials  $V_{nC}$ ,  $V_{CT}$  and  $V_{nT}$  are functions of the relative co-ordinates indicated as their arguments where

$$\vec{r}_{nT} = \vec{R} + \beta\vec{r}, \quad \beta = \frac{m_C}{m_P}, \quad (3.3)$$

$$\vec{r}_{CT} = \vec{R} - \alpha\vec{r}, \quad \alpha = \frac{m_n}{m_P}, \quad (3.4)$$

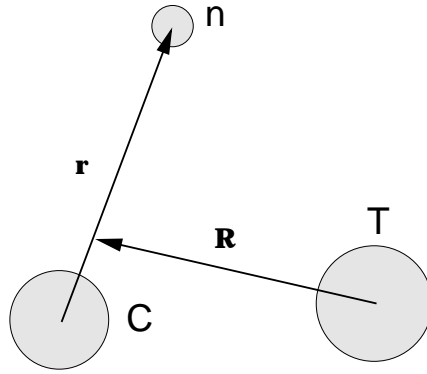


Fig. 1. Co-ordinates used in a 3-body model of a one neutron halo nucleus from a target  $T$ .

$$m_P = m_n + m_C. \quad (3.5)$$

These 2-body potentials depend only on relative co-ordinates and cannot excite the internal degrees of freedom of the core and the target nucleus. Such effects are taken into account implicitly by allowing  $V_{CT}$  and  $V_{nT}$  to be complex optical potentials which describe the relevant 2-body elastic scattering at correct relative velocity. For weakly bound halo nuclei the latter can be taken to be the relative velocity of the projectile and target.

It is important to appreciate the significance of eigenfunctions of this model  $H$ . They are functions  $\Psi(\vec{r}, \vec{R})$  which satisfy

$$H\Psi = E\Psi, \quad (3.6)$$

and describe that component of the true many-body wavefunction in which the target is in its ground state. The model eigenfunctions do have components in which the projectile is excited, but only those states which correspond to exciting the halo degrees of freedom including the continuum of break-up states. The model can therefore only describe cross sections for elastic scattering, certain inelastic excitations of the projectile, elastic break-up of the projectile in which the target and core are left in their ground states, and the total reaction cross section.

Possible states of the halo are eigenstates of  $H_{nC}$  and satisfy

$$\begin{aligned} (H_{nC} - \epsilon_i)\phi_i(\vec{r}) &= 0, \quad i = 0, 1, 2, \dots, \\ (H_{nC} - \epsilon_k)\phi_{\vec{k}}(\vec{r}) &= 0, \quad \epsilon_k = \frac{\hbar^2 k^2}{2\mu_{nC}}, \end{aligned} \quad (3.7)$$

where we have distinguished between discrete bound states labelled by  $i$  and the continuum states labelled by momentum  $\vec{k}$ . Transitions to the latter correspond to elastic break-up.

A standard approach to finding scattering state solutions to Eq. (3.6) is to look for solutions of the form of an expansion in the complete set of functions of  $\vec{r}$  defined in Eq. (3.7):

$$\begin{aligned} \Psi(\vec{R}, \vec{r}) &= \phi_0(\vec{r})\chi_0(\vec{R}) + \phi_1(\vec{r})\chi_1(\vec{R}) + \dots \\ &+ \int d\vec{k} \phi_{\vec{k}}(\vec{r})\chi_{\vec{k}}(\vec{R}). \end{aligned} \quad (3.8)$$

The functions  $\chi_i(\vec{R})$ ,  $\chi_{\vec{k}}(\vec{R})$  in Eq. (3.8) give the amplitudes for exciting the various halo states. All of them have the form of outgoing spherical waves at infinite  $R$  with amplitudes which determine the corresponding excitation cross sections. In the incident channel function  $\chi_0(\vec{R})$  there is in addition a plane wave describing the incident beam.

Following a standard procedure<sup>10)</sup> the  $\chi$  can be shown to satisfy a set of coupled differential equations which, if we ignore the continuum terms in Eq. (3.8), have the form

$$\begin{aligned} (E_0 - T_{\vec{R}} - V_{ii}(\vec{R}))\chi_i(\vec{R}) &= \sum_{j \neq i} V_{ij}(\vec{R})\chi_j(\vec{R}), \\ i, j &= 0, 1, \dots, \end{aligned} \quad (3.9)$$

where  $E_i = E - \epsilon_i$  and the coupling potentials  $V_{ij}(\vec{R})$  are given by

$$V_{ij} = \int d\vec{r} \phi_i^*(\vec{r}) [V_{nT}(\vec{R} + \beta\vec{r}) + V_{CT}(\vec{R} - \alpha\vec{r})] \phi_j(\vec{r}). \quad (3.10)$$

The coupling potentials describe the way tidal forces generated by the interactions between the components  $C$  and  $n$  of the projectile and the target can cause excitations of the projectile. It is the variation of the potentials on a scale of the order of the size of the projectile which generate terms with  $i \neq j$  which would otherwise vanish by the orthogonality of the  $\phi_j(\vec{r})$ .

When the continuum terms on the right-hand side of Eq. (3.8) are included the generalisation of Eq. (3.9) now includes coupling terms which couple discrete and continuum terms as well as terms coupling the continuum to itself. These terms involve coupling potentials like Eq. (3.10) but with at least one of the  $\phi_i(\vec{r})$  replaced by a  $\phi_{\vec{k}}(\vec{r})$ . These are the couplings which induce break-up of the halo and which are expected to play a prominent role in reactions involving halo nuclei.

One way of handling these equations when continuum couplings are important is to map the continuum onto a discrete square-integrable basis which is orthogonal to the bound states  $\phi_i$ . This is the approach pioneered by the Kyushu Group.<sup>6),7)</sup> This approach has been successfully applied the scattering of deuterons and other loosely bound nuclei but has difficulties when long range Coulomb couplings are included.<sup>8)</sup> Rather than discuss these results in detail we will discuss an approximation to the many-body scattering problem which is widely used, is sometimes much simpler to implement than the CDCC method and can provide interesting insights into the role of the continuum in the scattering of halo nuclei.

### 3.2. Adiabatic approximation

The adiabatic approximation as applied to the model of the last sub-section is based on the observation that at sufficiently high incident energy the halo degrees of freedom may be regarded as ‘frozen’ over the time needed for the projectile to traverse the target.<sup>\*)</sup> This does *not* mean that we assume that the projectile remains in the same eigenstate  $\phi_0$  of  $H_{nC}$ , but rather that the co-ordinate  $\vec{r}$  is frozen. This approximation is on the basis of Glauber’s theory of composite particle scattering,<sup>9)</sup> versions of which have been widely used in the analysis of reactions involving halo nuclei. The adiabatic approximation retains its usefulness, however, even when the other assumption of Glauber’s theory, i.e., the eikonal approximation, is not invoked.

We can get some insight into the validity of the adiabatic approximation and how it can be implemented by considering the time dependent version of Eq. (3.6)

$$H\Psi(\vec{R}, \vec{r}, t) = i\hbar\partial\Psi(\vec{R}, \vec{r}, t)/\partial t. \quad (3.11)$$

The substitution

$$\Psi = \exp(-i(H_{nC} - \epsilon_0)t/\hbar) \Phi, \quad (3.12)$$

transforms Eq. (3.11) into the equivalent form

$$(T_R + \epsilon_0 + V_{nT}(\vec{R} + \beta\vec{r}(t)) + V_{CT}(\vec{R} - \beta\vec{r}(t)))\Phi = i\hbar\partial\Phi/\partial t, \quad (3.13)$$

---

<sup>\*)</sup> It is unfortunate that the term adiabatic is sometimes used to denote exactly the opposite approximation, e.g., in the Coulomb excitation literature. Here we follow the usage in Ref. 10).

where the term in  $H_{nC}$  has been removed at the expense of a time dependent  $\vec{r}(t)$  satisfying

$$\vec{r}(t) = \exp(i(H_{nC} - \epsilon_0)t/\hbar) r \exp(-i(H_{nC} - \epsilon_0)t/\hbar). \quad (3.14)$$

The adiabatic approximation replaces  $r(\vec{t})$  by  $r(\vec{0}) = \vec{r}$  in Eq. (3.13). A sufficient condition for this to be accurate over the collision time  $t_{\text{coll}}$  is

$$(H_{nC} - \epsilon_0)t_{\text{coll}}/\hbar \ll 1. \quad (3.15)$$

When this adiabatic condition is satisfied, stationary state solutions of Eq. (3.13) satisfy

$$\left(T_R + V_{nT}(\vec{R} + \beta\vec{r}) + V_{CT}(\vec{R} - \beta\vec{r})\right)\Phi = E_K\Phi, \quad (3.16)$$

where  $E_K = E - \epsilon_0$  is the incident kinetic energy and we have assumed a time dependent factor  $\exp(-iEt/\hbar)$  for times satisfying Eq. (3.15).

In Eq. (3.16)  $\vec{r}$  is no longer a dynamical variable but a parameter. The 3-body problem we started with has been reduced to a set of 2-body problems, one for each value of  $\vec{r}$ . The resulting solution  $\phi^{\text{Adia}}(\vec{R}, \vec{r})$  is a superposition of all the projectile states  $(\phi_i(\vec{r}), \phi_{\vec{k}}(\vec{r}))$ .

The adiabatic approximation to the transition amplitude to a particular projectile state is calculated by projecting onto that state and examining the coefficient of the outgoing wave for  $R$  asymptotically large. If  $f(\theta, \phi, \vec{r})$  is the scattering amplitude in the direction  $\theta, \phi$  calculated from Eq. (3.16) for a fixed value of  $\vec{r}$ , then the scattering amplitude for exciting state  $i$  is

$$f_{i0} = \int d\vec{r} \phi_i^*(\vec{r}) f(\theta, \phi, \vec{r}) \phi_0(\vec{r}). \quad (3.17)$$

Examples of the application of this method to composite particle scattering including several frozen degrees of freedom can be found in Refs. (11), (12), (15), (13), (14). When the 2-body scattering problem Eq. (3.16) is solved using the additional assumption of straight line trajectories in  $\vec{R}$ -space the results are equivalent to Glauber's<sup>9)</sup> theory. Calculations along these lines<sup>1), 2), 30), 16), 17), 33)</sup> have been of great importance in the interpretation of reaction cross sections for halo nuclei in terms of nuclear sizes. Some of the earlier calculations used a further approximation to Glauber's many body theory known variously as the 'optical limit', the 'static limit', or the 'folding model'. It has been proved recently<sup>19)</sup> that for a given halo wavefunction the 'folding model' always overestimates the total reaction cross section for strongly absorbed particles. Published complete Glauber calculations<sup>16), 17), 33)</sup> are consistent with this theorem.

It is clearly desirable to convert the adiabatic condition Eq. (3.15) into a quantitative estimate expressed in terms of the parameters of the collision process of interest and to devise methods of calculating the leading corrections to the adiabatic scattering amplitudes. It is clear that Eq. (3.15) requires small projectile excitation energies (slow halo degrees of freedom) and high incident energies (short collision times). Qualitative estimates along these lines can be found in Refs. (9), (23), (24), and

some progress has been made in deriving correction terms for transfer reactions<sup>20)</sup> and elastic scattering.<sup>25)</sup> Here we shall assume that the adiabatic approximation is adequate and confine ourselves to the scattering of halo nuclei at energies for which a simple estimate indicates there is a good case for this to be a valid starting point.

The adiabatic approximation can also be regarded as an approximate solution of the coupled equations (3.9) when all the channel energies  $E_i$  are assumed to be degenerate and equal to  $E_0$ . Multiplying the  $i$ th equation by  $\phi_i(\vec{r})$ , summing up all the equations over  $i$  using the completeness of the  $\phi_i(\vec{r})$ , one obtains an equation equivalent to Eq. (3.16) with  $\phi$  identified as  $\sum \phi_i \chi_i$ . This derivation does not give an immediate indication of the conditions for the validity of the approximation.

### 3.3. Special cases

Implementation of the adiabatic approximation requires the calculation of scattering solutions  $\phi^{\text{Adia}}(\vec{R}, \vec{r})$  of Eq. (3.16). Equation (3.16) for fixed  $\vec{r}$  is equivalent to a 2-body problem in a non-central potential (even if  $V_{nT}$  and  $V_{CT}$  are themselves central) and an exact solution requires the solution of coupled equations.<sup>11), 12), 15)</sup>

There are 2 cases when an enormous simplification occurs:

1. When  $\phi^{\text{Adia}}(\vec{R}, \vec{r})$  is required at the point  $r = 0$  only. Equation (3.16) then reduces to a 2-body central force problem in the potential  $V_{nT}(R) + V_{CT}(R)$ . This insight has been exploited<sup>11), 21), 20)</sup> to give a theory of deuteron stripping and pick-up which includes deuteron break-up effects in a simple way.
2. When one of the interactions  $V_{nT}$  and  $V_{CT}$  between the constituents of the projectile and the target is zero.<sup>22)</sup> We shall refer to this special case as ‘the recoil model’ because the only way the projectile can be excited or broken up is through recoil of the core following scattering by the target. Note that the other 2 interactions  $V_{nC}$  and  $V_{CT}$  can be of arbitrary strength or range and may include Coulomb terms.

In the second case the exact solution of Eq. (3.16) corresponding to a projectile in its ground state  $\phi_0$  incident with momentum  $\vec{K}$  on a target  $T$  is<sup>22), 24), 23)</sup>

$$\phi_{\vec{K}}^{(+)\text{Adia}}(\vec{r}, \vec{R}) = \phi_0(\vec{r}) e^{i\alpha\vec{K}\cdot\vec{r}} \chi_{\vec{K}}^{(+)}(\vec{R} - \alpha\vec{r}), \quad (3.18)$$

where  $\chi_{\vec{K}}^{(+)}$  is a distorted wave which describes the scattering of a particle of mass  $\mu_{PT}$  (the projectile-target reduced mass) from the potential  $V_{CT}$ , i.e.,

$$\begin{aligned} [T_{R'} + V_{CT}(\vec{R}')] \chi_{\vec{K}}^{(+)}(\vec{R}') &= E_K \chi_{\vec{K}}^{(+)}(\vec{R}'), \\ \chi_{\vec{K}}^{(+)}(\vec{R}')_{R' \rightarrow \infty} &\rightarrow \exp(i\vec{K} \cdot \vec{R}') + f_{CT} \exp(iKR')/R'. \end{aligned} \quad (3.19)$$

Note that in Eq. (3.18) the distorted wave has the argument  $(\vec{R} - \alpha\vec{r})$ , which is just the  $C$ - $T$  separation. The distorted wave corresponds to a model in which all effects due to the halo neutron are ignored apart from its contribution to the mass of the projectile. In the following we will refer to this limit as the scattering of a ‘no halo’ projectile.

We emphasise that the three-body wavefunction, Eq. (3.18), includes components which describe break-up and excitations of the projectile. This is clear from

the complicated dependence on  $\vec{r}$ , through the argument of  $\chi_{\vec{K}}^{(+)}$  and the exponential factor  $\exp(i\alpha\vec{K}\cdot\vec{r})$  which will result in a non-vanishing overlap with any of the states  $(\phi_i(\vec{r}), \phi_{\vec{k}}(\vec{r}))$ .

### 3.4. Applications of the adiabatic ‘recoil model’

The exact elastic scattering transition amplitude for the projectile, from initial state  $\vec{K}$  into final state  $\vec{K}'$ , is

$$T_{\text{el}}(\vec{K}', \vec{K}) = \int d\vec{r} \int d\vec{R} \phi_0^*(\vec{r}) e^{-i\vec{K}'\cdot\vec{R}} V_{CT}(\vec{R} - \alpha\vec{r}) \Psi_{\vec{K}}^{(+)}(\vec{r}, \vec{R}), \quad (3\cdot20)$$

where  $\Psi_{\vec{K}}^{(+)}(\vec{r}, \vec{R})$  is the exact scattering state solution of Eq. (3\cdot6).

Using the adiabatic approximation to  $\Psi_{\vec{K}}^{(+)}$ , Eq. (3\cdot18), and making the change of variable from  $\vec{R}$  to  $\vec{R}' = \vec{R} - \alpha\vec{r}$  this factorises as

$$T_{\text{el}}(\vec{K}', \vec{K}) = \left[ \int d\vec{r} |\phi_0(\vec{r})|^2 e^{i\alpha(\vec{K} - \vec{K}')\cdot\vec{r}} \right] \left[ \int d\vec{R}' e^{-i\vec{K}'\cdot\vec{R}'} V_{CT}(\vec{R}') \chi_{\vec{K}}^{(+)}(\vec{R}') \right]. \quad (3\cdot21)$$

The second integral here is just the transition amplitude  $T_{\text{no halo}}(\vec{K}', \vec{K})$  for a ‘no halo’ projectile scattering by the core-target potential  $V_{CT}$ . The same result for  $T_{\text{el}}$  is obtained by examining the asymptotic form of Eq. (3\cdot18) in the elastic channel.

The effects of projectile excitation and structure in Eq. (3\cdot21) arise entirely through the first integral, the form factor

$$F(\vec{Q}) = \int d\vec{r} |\phi_0(\vec{r})|^2 \exp(i\vec{Q}\cdot\vec{r}), \quad (3\cdot22)$$

where  $\vec{Q} = \alpha(\vec{K} - \vec{K}')$ . The corresponding elastic scattering differential cross section is therefore

$$\left( \frac{d\sigma}{d\Omega} \right)_{\text{el}} = |F(\vec{Q})|^2 \times \left( \frac{d\sigma}{d\Omega} \right)_{\text{no halo}}, \quad (3\cdot23)$$

where  $(d\sigma/d\Omega)_{\text{no halo}}$  is the cross section for a projectile, with mass  $\mu$ , scattering by the core-target interaction and is therefore very closely related to the experimental core-target elastic scattering.

The importance of Eq. (3\cdot23) is that it clarifies the relevant scattering angles and incident energies at which a halo of a given size and structure will be manifest as a deviation from the scattering due to a projectile which does not have the spatial extension associated with a loosely bound halo particle.

Equation (3\cdot23) is reminiscent of factorisations which occur in electron scattering when Born approximation and approximate distorted wave theories are used. Note, however, that the present analysis does not involve Born approximation in any sense. Only if all intermediate states are included the second and higher order terms in the Born series factorise in this way.<sup>24)</sup> The same argument obtains for the factorisation of the wavefunction in Eq. (3\cdot18).

<sup>11</sup>Be is a good example of a binary, <sup>10</sup>Be+*n*, single neutron halo nucleus and <sup>19</sup>C is also a single neutron halo candidate.<sup>26)</sup> Both systems have small  $\alpha = m_n/m_P$  ratios. For <sup>11</sup>Be+<sup>12</sup>C, there are small angle elastic scattering data<sup>27)</sup> for both the <sup>10</sup>Be

core and the  $^{11}\text{Be}$  composite, but at energies of 59.4 MeV/A and 49.3 MeV/A, respectively. Ideally these data are required at the same energy per nucleon to provide the necessary information on  $V_{CT}$ , which is an essential ingredient in applications of Eq. (3.23).

According to Eq. (3.23) the formfactor  $|F(Q)|^2$ , which multiplies the point particle cross section, reflects the modifications to the scattering due to the composite nature of the projectile. In Fig. 2 we show calculated squared formfactors as a function of the centre-of-mass angles which are appropriate for the elastic scattering of  $^{11}\text{Be}$  (upper part) and  $^{19}\text{C}$  (lower part) from  $^{12}\text{C}$  at 49.3 MeV/A and 30 MeV/A, respectively. These calculations demonstrate the sensitivity of the formfactor to the halo properties. Conversely, they demonstrate the information about the halo-core relative motion wavefunction which is available in principle from halo nucleus elastic scattering data.

The strong deviations from unity shown in Fig. 2 reflect in momentum space the long exponential tails of the halo wavefunctions we discussed in §2. In the notation of that section, a neutron wavefunction with a  $\lambda$ -value corresponding to a typical non-halo nucleus the formfactor would hardly deviate at all from unity over the angular range of Fig. 2.

For  $^{11}\text{Be}$ , the halo is seen to result in a reduction in the elastic differential

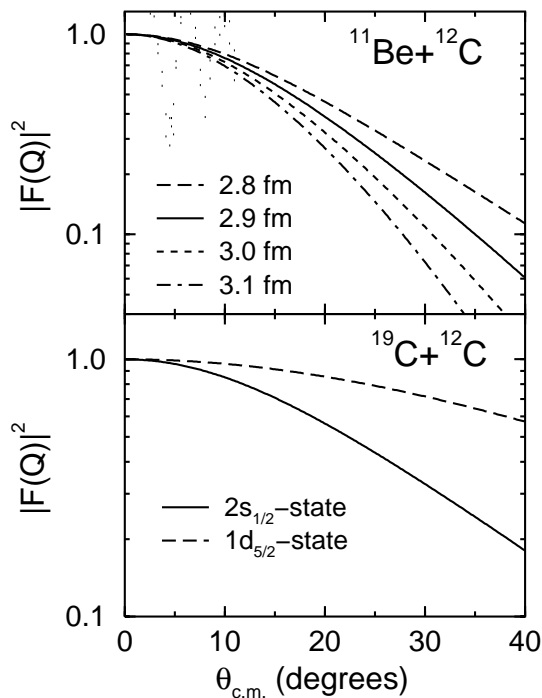


Fig. 2. Calculated  $|F(Q)|^2$ , as a function of centre-of-mass scattering angle for the elastic scattering of  $^{11}\text{Be}$  (upper part) and  $^{19}\text{C}$  (lower part) from  $^{12}\text{C}$  at 49.3 MeV/A and 30 MeV/A, respectively.

cross section by a factor of between 2 and 4 at  $20^\circ$ , compared to that for ‘no halo’ scattering. There is also a significant sensitivity to the assumed rms separation of the valence and core particles.

For  $^{19}\text{C}$ , the squared formfactors which result from a pure  $2s_{1/2}$  (solid curve) or  $1d_{5/2}$  (dashed curve) neutron state are shown. The departures from ‘no halo’ scattering are predicted to be significantly different for a  $2s_{1/2}$  and  $1d_{5/2}$  valence neutron, with almost a factor of 2 difference in the cross sections at  $20^\circ$ . We note that, although the leading term in the expansion of the formfactor about  $Q = 0$  gives a deviation from unity proportional to the mean squared separation of the core and valence particles in the projectile, the values of  $Q$  which enter in the examples above are such that this leading order term is inadequate and there is sensitivity to higher order moments except at the very smallest angles.

For  $^{11}\text{Be}$  the wavefunctions were taken to be pure  $2s_{1/2}$  neutron single particle states, with separation energy 0.503 MeV, calculated in a central Wood-Saxon potential.<sup>28)</sup> By changing the binding potential geometry we generate  $^{11}\text{Be}$  composites with different rms matter radii and hence  $|F(Q)|^2$ . For  $^{19}\text{C}$  the ground state structure is presently uncertain with speculations of it being a pure  $2s_{1/2}$  state,  $1d_{5/2}$  state or a linear combination of such configurations.<sup>29)</sup> The neutron separation energy was 0.240 MeV.

Figure 3 shows the elastic differential cross section angular distributions (ratio to Rutherford) for  $^{11}\text{Be}+^{12}\text{C}$  scattering at 49.3 MeV/A calculated with a number of different models of the scattering mechanism.

The dashed curve shows the ‘no halo’ projectile differential cross section  $(d\sigma/d\Omega)_{\text{no halo}}$  calculated using the core-target potential. It might be expected that

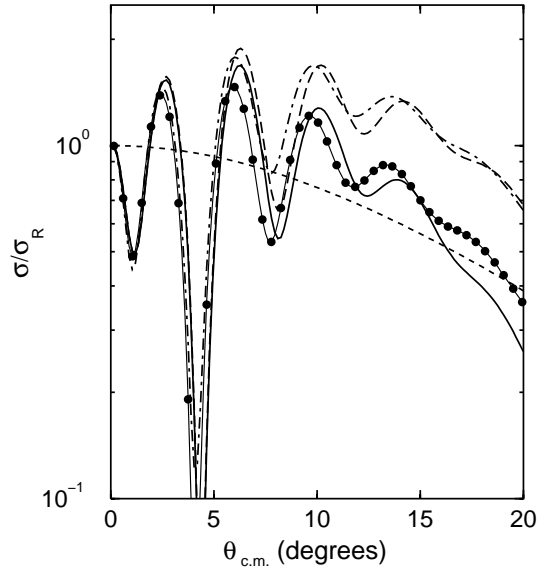


Fig. 3. Calculated elastic differential cross section angular distributions (ratio to Rutherford) for  $^{11}\text{Be}+^{12}\text{C}$  scattering at 49.3 MeV/A. The curves are discussed in the text.

the main effect of the extended size of the projectile could be accounted for by calculating the scattering by a potential  $V_{\text{fold}}(R)$  which averages  $V_{nT}(\vec{R} + \beta\vec{r}) + V_{CT}(\vec{R} - \alpha\vec{r})$  over the probability density for  $\vec{r}$  predicted by the ground state halo density.

$$V_{\text{fold}}(R) = \int d\vec{r} [V_{nT}(\vec{R} + \beta\vec{r}) + V_{CT}(\vec{R} - \alpha\vec{r})] |\phi_0(r)|^2. \quad (3\cdot24)$$

The dot-dashed curve in Fig. 3 shows the cross section calculated using the folding model interaction, Eq. (3·24). The similarity of the folding and ‘no halo’ calculations makes clear that the effects associated simply with folding the core and valence particle interactions over the size of the halo are relatively minor compared with the effects taken into account in the solid curve. The latter is obtained using the result Eq. (3·23) with the squared formfactor shown by the short dashed line (the 2.9 fm rms case of Fig. 2).

The physical difference between the theory which produces the solid line and the ‘folding’ result is that the former does not assume that the projectile remains in its ground state during the scattering but correctly takes into account (insofar as the adiabatic approximation is adequate) the large projectile excitation and break-up effects induced by the target. It is remarkable that such complicated multistep processes are fully accounted for by Eq. (3·23) when the interaction between the halo and the target is ignored. Note, however, that at small angles the ‘folding’ diffraction pattern is shifted to smaller angles as one would expect for the more spatially extended potential of Eq. (3·24).

We recall that the special case under discussion ignores the interaction between the valence neutron and the target. In fact this interaction is not negligible and must be taken into account in a detailed comparison with experiment. This is not a difficulty since exact adiabatic calculations which include the interaction between all the halo particles and the target are possible for both two and three-body projectile systems.<sup>15), 14)</sup> Such calculations have also been carried out for 4- and 5-body projectiles within the eikonal approximation.<sup>31), 32)</sup>

In Fig. 4 we show the results of such adiabatic calculations for  $^{11}\text{Be} + ^{12}\text{C}$  scattering at 49.3 MeV/A. These include the neutron+ $^{12}\text{C}$  optical potential tabulated in Ref. 34), and correspond to the four  $^{11}\text{Be}$  wavefunctions with different rms radii discussed in connection with Fig. 2. The data are from Ref. 27). We note that the behavior of the cross sections expected on the basis of the formfactors of Fig. 2 and the insights the ‘recoil model’ provides are not affected in any major way by the neutron-target interaction. These results suggest that elastic scattering data of sufficient quality could yield independent information on halo structures.

The full circle symbols in Fig. 3 are also full adiabatic model calculation including  $V_{nT}$ . They can be compared with the solid line results which are also adiabatic but do not include  $V_{nT}$ . The agreement is reasonable and suggests that  $V_{CT}$  in this system dominates, although the effects of the valence neutron-target interaction are not negligible.

The ‘recoil model’ teaches us that halo nucleus elastic scattering angular distributions are strongly affected by projectile excitation channels and the spatial size of the halo. These effects are principally manifest through a formfactor which depends

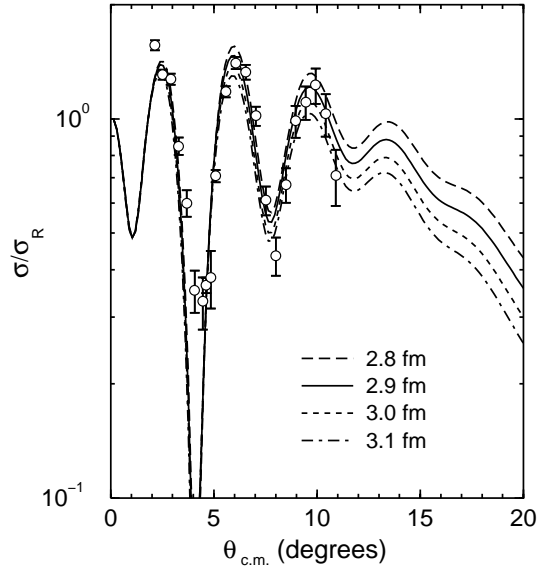


Fig. 4. Calculated elastic differential cross section angular distributions (ratio to Rutherford) for  $^{11}\text{Be}+^{12}\text{C}$  scattering at 49.3 MeV/A calculated using the adiabatic approximation and including the neutron-target interaction.

only on the halo ground state wavefunction and whose square multiplies the ‘no halo’ cross section. The latter is defined to be the cross section for a particle with the mass of the projectile but which interacts with the target through the core-target potential with no folding in of the halo density. This potential is in principle to be obtained from core-target scattering at the same energy per nucleon as that of the halo nucleus scattering of interest. In fact to a good approximation at the energy used in Fig. 2 the ‘no halo’ cross section can be evaluated directly from the core-target cross section at the same energy per nucleon and momentum transfer.

#### §4. Other applications of the ‘recoil model’

We have already mentioned the application of the adiabatic approximation to the calculation of reaction cross sections for halo nuclei in §3.2. The approximation has also been widely used to treat deuteron break-up effects in stripping and pick-up reactions (see Refs. 20), 39) and references therein). The special case of the ‘recoil model’ has had some other interesting recent applications.

##### 4.1. Coulomb break-up of neutron halo nuclei

One situation when the neglect of the interaction between the halo neutron and the target can be justified is when Coulomb forces dominate. We will now explain how the ‘recoil model’ can be used as the starting point of a non-perturbative quantum mechanical theory of the Coulomb break-up of neutron halo nuclei.<sup>36)–38)</sup>

Some care is required in using the adiabatic wavefunction to calculate break-

up amplitudes. The explicit form of the solution Eq. (3.18) makes it clear that at large core-neutron separations,  $r \rightarrow \infty$ , the presence of the factor  $\phi_0$  means that, independently of the details of the 3-body Hamiltonian,  $\phi_{\vec{K}}^{(+)\text{Adia}}(\vec{r}, \vec{R})$  vanishes exponentially. The large  $r$  region is where one would expect to look for break-up flux and therefore  $\phi_{\vec{K}}^{(+)\text{Adia}}(\vec{r}, \vec{R})$  cannot be used to calculate break-up amplitudes by looking at its asymptotic form.

It follows that to use the three-body wavefunction of Eq. (3.18) to calculate a Coulomb break-up amplitude we must restrict its use to regions of the six-dimensional  $(\vec{r}, \vec{R})$  space where  $r$  is finite. In particular, we do not attempt to extract the break-up amplitude from the asymptotics of our approximate adiabatic solution. Reference 36) proceeds instead as follows.

We first rewrite the *exact* three-body Schrödinger equation of Eq. (3.6), prior to having made any adiabatic approximation, as

$$\left[ E - T_{\vec{R}_n} - T_{\vec{R}_C} - V_{CT}(\vec{R}_C) \right] \Psi_{\vec{K}}^{(+)}(\vec{r}, \vec{R}) = V_{nC}(\vec{r}) \Psi_{\vec{K}}^{(+)}(\vec{r}, \vec{R}), \quad (4.1)$$

where  $T_{\vec{R}_n}$  and  $T_{\vec{R}_C}$  are the kinetic energies in the co-ordinates  $\vec{R}_n$  and  $\vec{R}_C$ . These Jacobi co-ordinates are defined so that  $\vec{R}_n$  connects  $n$  with the centre-of-mass of  $C$  and  $T$ , and  $\vec{R}_C$  is the  $C$ - $T$  separation (see Fig. 5). They are particularly suitable when  $V_{nT} = 0$ .

The right-hand side of Eq. (4.1) requires only finite separations  $\vec{r}$ , and therefore we can justifiably evaluate it using the adiabatic wavefunction  $\phi_{\vec{K}}^{(+)\text{Adia}}(\vec{r}, \vec{R})$  as a good approximation to  $\Psi_{\vec{K}}^{(+)}$ . This procedure yields the inhomogeneous equation

$$\left[ E - T_{\vec{R}_n} - T_{\vec{R}_C} - V_{CT}(\vec{R}_C) \right] \hat{\Psi}_{\vec{K}}^{(+)}(\vec{r}, \vec{R}) = V_{nC}(\vec{r}) \phi_{\vec{K}}^{(+)\text{Adia}}(\vec{r}, \vec{R}). \quad (4.2)$$

For a given adiabatic wavefunction Eq. (4.2) can be solved using Green function techniques to give a solution which has the correct 3-body asymptotics<sup>36)</sup> and from which an expression for the break-up amplitude into any final state can be read off. The break-up amplitude calculated in this way for a three-body final state with Jacobi momenta  $\vec{q}_C$  and  $\vec{q}_n$  corresponding to  $\vec{R}_n$  and  $\vec{R}_C$ , is found to be<sup>36)</sup>

$$\bar{T}_{\text{AD}}(\vec{q}_n \vec{q}_C, \vec{K}) = \left\langle e^{i\vec{q}_n \cdot \vec{R}_n} \chi_{\vec{q}_C}^{(-)}(\vec{R}_C) | V_{nC}(\vec{r}) | \bar{\Psi}_{\vec{K}}^{(+)}(\vec{r}, \vec{R}) \right\rangle, \quad (4.3)$$

where  $\chi_{\vec{q}_C}^{(-)}$  is a Coulomb distorted wave with in-going scattered waves describing the scattering of the outgoing core by the target.

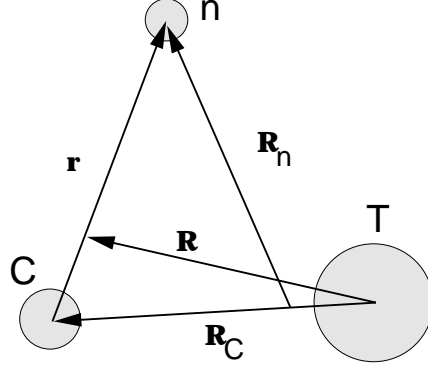


Fig. 5. Definition of the co-ordinate system adopted for the core, valence, and target three-body system.

It is shown in Ref. 36) that the break-up amplitude  $\bar{T}_{AD}$  of Eq. (4.3) is exactly the same as the expression obtained by using the adiabatic wavefunction directly in the exact post-form transition amplitude.

Note that although the adiabatic approximation neglects the projectile excitation energy in the calculation of the adiabatic three-body wavefunction  $\bar{\Psi}_{\vec{K}}^{(+)}$ , this does not mean that the break-up amplitude is calculated using the zero adiabaticity parameter  $\xi = 0$  limit, of semi-classical theories.<sup>40)</sup> As the analysis above shows,  $\bar{T}_{AD}$  includes a final state wavefunction with the correct kinematics and excitation energies required by energy conservation, unlike analogous  $\xi = 0$  semi-classical calculations.

#### 4.2. Break-up transition amplitude

It is shown in Ref. 36) that the amplitude  $\bar{T}_{AD}$  of Eq. (4.3) factorises exactly as

$$\begin{aligned} \bar{T}_{AD}(\vec{q}_n \vec{q}_C, \vec{K}) &= \left[ \int d\vec{r} e^{-i\vec{P}_n \cdot \vec{r}} V_{nC}(\vec{r}) \phi_0(\vec{r}) \right] \left[ \int d\vec{R}_C e^{-i\vec{Q}_n \cdot \vec{R}_C} \chi_{\vec{q}_C}^{(-)*}(\vec{R}_C) \chi_{\vec{K}}^{(+)}(\vec{R}_C) \right] \\ &= \langle \vec{P}_n | V_{nC} | \phi_0 \rangle \langle \vec{Q}_n, \chi_{\vec{q}_C}^{(-)} | \chi_{\vec{K}}^{(+)} \rangle, \end{aligned} \quad (4.4)$$

where we have defined  $\vec{P}_n = \vec{q}_n - \alpha \vec{K}$  and  $\vec{Q}_n = \frac{m_T}{m_T + m_C} \vec{q}_n$ .

The two factors in Eq. (4.4) separate out the structure and dynamical parts of the calculation. The overlap of the three continuum functions,  $\langle \vec{Q}_n, \chi_{\vec{q}_C}^{(-)} | \chi_{\vec{K}}^{(+)} \rangle$ , can be evaluated in closed form and expressed in terms of the bremsstrahlung integral.<sup>36)</sup> This factor now contains all the dynamics of the break-up process and is readily calculated for given incident and outgoing momenta in terms of the charges and masses of  $C$  and  $T$ .

The structure of the projectile enters through the vertex function  $\langle \vec{P}_n | V_{nC} | \phi_0 \rangle$  and is also simply evaluated given any structure model for the projectile. In Coulomb dissociation, momentum can be transferred to the valence particle only by virtue of its interaction  $V_{nC}$  with the core. Since the term  $\alpha \vec{K}$  in  $\vec{P}_n$  is the fraction of the incident momentum of the projectile which is carried by the valence particle, this structure vertex displays explicitly this momentum transfer from the ground state via  $V_{nC}$ .

Without any approximation additional to the adiabatic assumption, Eq. (4.4) allows a fully finite-range treatment of the core-neutron particle interaction  $V_{nC}$ . The theory is thus applicable to projectiles with any ground state orbital angular momentum structure, and also includes break-up contributions from all contributing Coulomb multipoles and relative orbital angular momenta between the neutron and core fragments. Unlike DWBA theories it includes the initial and final state interactions  $V_{CT}$  and  $V_{nC}$  to all orders.

The theory has been successfully applied to the break-up of high energy deuterons in the forward direction,<sup>36), 41)</sup> and with appropriate generalisation, to the Coulomb break-up of one- and two-neutron halo nuclei.<sup>37), 38)</sup> Here we briefly mention the case of deuteron break-up.

The  $(d, pn)$  elastic break-up data have been measured at the RIKEN Accelerator Research Facility, Saitama, at 140 and 270 MeV, and at the Research Centre for

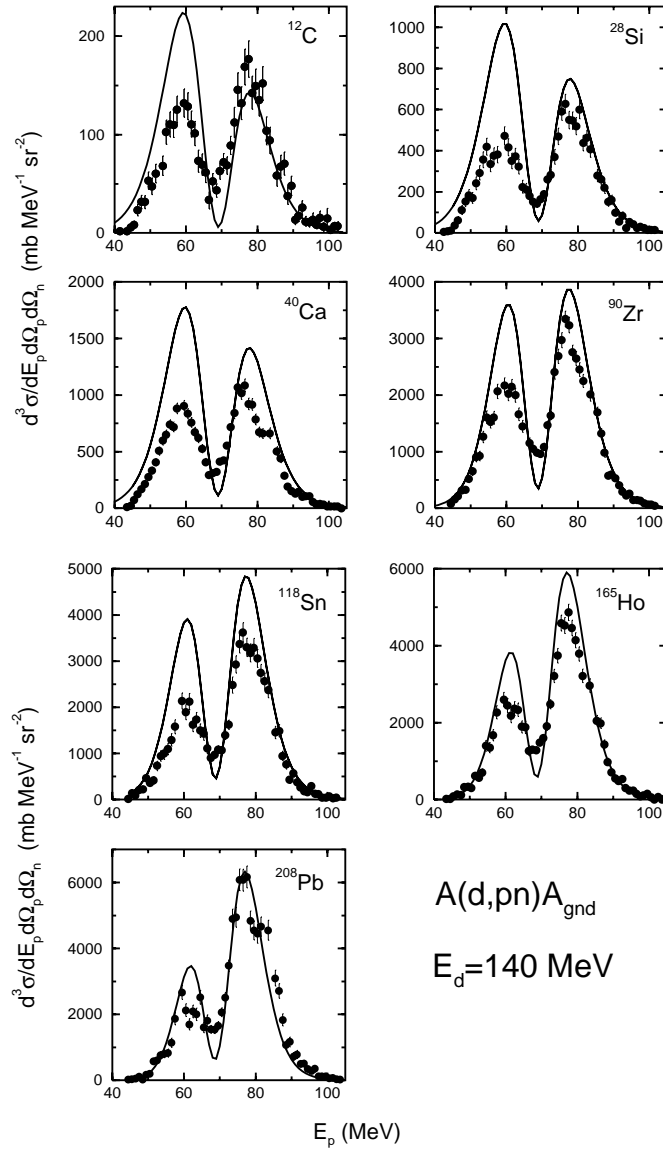


Fig. 6. Experimental and calculated adiabatic model (solid curves) triple differential cross sections for deuteron break-up near  $0^\circ$  in the laboratory frame at  $E_d = 140$  MeV. The calculations are averaged over the neutron and proton solid angles actually used in the experiment. The data are from Ref. 41).

Nuclear Physics (RCNP), Osaka, at 56 MeV in a kinematical condition of  $\theta_p \approx \theta_n \approx 0^\circ$ . The targets were  $^{12}\text{C}$ ,  $^{28}\text{Si}$ ,  $^{40}\text{Ca}$ ,  $^{90}\text{Zr}$ ,  $^{118}\text{Sn}$ ,  $^{165}\text{Ho}$  and  $^{208}\text{Pb}$  at  $E_d=140$  and 270 MeV and  $^{12}\text{C}$ ,  $^{40}\text{Ca}$ ,  $^{90}\text{Zr}$ , and  $^{208}\text{Pb}$  at  $E_d=56$  MeV.

The calculations and data at 140 MeV are compared in Fig. 6 for all measured targets. The errors shown in the figure are statistical only. The solid lines show the

elastic break-up cross sections, as a function of the detected (laboratory) proton energy, calculated using Eq. (4.4). The overall agreement of the calculated magnitudes,  $Z_T$ -dependence, and the proton energy dependence, with the data is good and improves with increasing target charge. The factor of 40 increase in the magnitudes of the measured cross sections in going from  $^{12}\text{C}$  to  $^{208}\text{Pb}$  is seen to be well reproduced as a function of  $Z_T$ . Figure 6 does not, however, reveal the complex way that the calculated cross sections are built up in the integrations over the experimental solid angle acceptances. We refer to Refs. 36) and 41) for these crucial considerations and for a full discussion of the results at all 3 incident energies.

We emphasise again that these calculations are non-perturbative and fully quantum mechanical. They are based on a theory which is very different from the DWBA both in principle and in terms of the numerical results obtained. These differences are discussed in detail in Ref. 36). Final state interactions between the outgoing fragments are fully taken into account, apart from the nuclear interaction between the neutron and the target. The nuclear interaction between the neutron and the proton is accounted for to all orders.

The results of Refs. 36) and 41) are consistent with an underlying physical picture in which Coulomb break-up is the dominant mechanism. There are, however, indications of a missing and interfering contribution, particularly on the lighter targets which may result from break-up by the nuclear forces between the projectile and the target which are ignored in the model of Refs. 36) and 41).

#### 4.3. Deuteron stripping and pick-up on halo nuclei

We have already mentioned the use of the adiabatic approximation to treat multi-step processes via deuteron break-up channels in stripping and pick-up reactions. This is special case 1 of §3.3. A recent development has been to use the adiabatic approximation to additionally treat excitations of the final nucleus in a  $(d, p)$  reaction in which the final nucleus is a halo nucleus. It is shown in Ref. 39) how the simplicity of the ‘recoil model’ can be exploited to give a very convenient way of evaluating what would otherwise be a very complicated multi-channel calculation. See also Ref. 25) for an application to recent  $^{11}\text{Be}(p, d)^{10}\text{Be}$  data from GANIL.<sup>42)</sup>

## §5. Conclusions

I hope I have convinced you of the fascination of nuclear reactions with halo and other weakly bound nuclei. New experiments are giving a new challenge to theory and our Group in Surrey is working very hard to meet this challenge. I hope I have also convinced you that the adiabatic treatment of the halo degrees of freedom provides a useful insight into the physics involved.

A particular challenge to theory is to understand and evaluate the leading corrections to the adiabatic theory and to learn how to apply them to transfer and break-up reactions. There is also a need to understand how the few-body models of reactions described here can be related to the underlying many-fermion structure of the halo nucleus.

## Acknowledgements

I am grateful to Professor H. Horiuchi and the Organising Committee for giving me the honour of participating in the Nishinomiya Yukawa Symposium and to the Mayor and City of Nishinomiya for their very generous hospitality.

## References

- 1) I. Tanihata, H. Hamagaki, O. Hashimoto, S. Nagamiya, Y. Shida, N. Yoshikawa, O. Yamakawa, K. Sugimoto, T. Kobayashi, D. E. Greiner, N. Takahashi and Y. Nojiri, *Phys. Lett.* **B160** (1985), 380.
- 2) I. Tanihata, T. Kobayashi, O. Yamakawa, T. Shimoura, K. Ekuni, K. Sugimoto, N. Takahashi, T. Shimoda and H. Sato, *Phys. Lett.* **B206** (1988), 592.
- 3) I. Tanihata, H. Hamagaki, O. Hashimoto, Y. Shida, N. Yoshikawa, K. Sugimoto, O. Yamakawa, T. Kobayashi and N. Takahashi, *Phys. Rev. Lett.* **55** (1985), 2676.
- 4) P. G. Hansen, A. S. Jensen and B. Jonson, *Annu. Rev. Nucl. Part. Sci.* **45** (1995), 591.
- 5) I. J. Thompson, B. V. Danielin, V. D. Efros, J. S. Vaagen, J. M. Bang and M. V. Zhikov, *Phys. Rev.* **C61** (2000), 024318.
- 6) M. Kamimura, M. Yahiro, Y. Iseri, H. Kameyama, Y. Sakuragi and M. Kawai, *Prog. Theor. Phys. Suppl.* No. 89 (1986), 1.
- 7) N. Austern, Y. Iseri, M. Kamimura, M. Kawai, G. Rawitscher and M. Yahiro, *Phys. Rep.* **154** (1987), 125.
- 8) F. M. Nunes and I. J. Thompson, *Phys. Rev.* **C59** (1999), 2652.
- 9) R. J. Glauber, in *Lectures in Theoretical Physics*, ed. W. E. Brittin (Interscience, New York, 1959), vol. 1, p. 313.
- 10) G. R. Satchler, *Direct Nuclear Reactions* (Oxford University Press, Oxford, 1983).
- 11) R. C. Johnson and P. J. R. Soper, *Phys. Rev.* **C1** (1970), 976.
- 12) H. Amakawa, S. Yamaji, A. Mori and K. Yazaki, *Phys. Lett.* **B82** (1979), 13.
- 13) J. S. Al-Khalili and R. C. Johnson, *Nucl. Phys.* **A546** (1992), 622.
- 14) J. A. Christley, J. S. Al-Khalili, J. A. Tostevin and R. C. Johnson, *Nucl. Phys.* **A624** (1997), 275.
- 15) I. J. Thompson, Computer Programme ADIA, Daresbury Laboratory Report (1984), unpublished.
- 16) J. S. Al-Khalili and J. A. Tostevin, *Phys. Rev. Lett.* **76** (1996), 3903.
- 17) J. S. Al-Khalili, I. J. Thompson and J. A. Tostevin, *Phys. Rev.* **C54** (1996), 1843.
- 18) J. A. Tostevin, R. C. Johnson and J. S. Al-Khalili, *Nucl. Phys.* **A630** (1998), 340c.
- 19) R. C. Johnson and C. J. Goebel, *Phys. Rev. C*, in press.
- 20) A. Laid, J. A. Tostevin and R. C. Johnson, *Phys. Rev.* **C48** (1993), 1307.
- 21) J. D. Harvey and R. C. Johnson, *Phys. Rev.* **C3** (1971), 636.
- 22) R. C. Johnson, J. S. Al-Khalili and J. A. Tostevin, *Phys. Rev. Lett.* **79** (1997), 2771.
- 23) R. C. Johnson, *J. of Phys.* **G24** (1998), 1583.
- 24) R. C. Johnson, in *Proc. Eur. Conf. On Advances in Nuclear Physics and Related Areas, Thessaloniki, Greece, July 8-12, 1997*, ed. D. M. Brink, M. E. Grypeos and S. E. Massen (Giahoudi-Giapouli, Thessaloniki, 1999), p. 156.
- 25) R. C. Johnson, J. S. Al-Khalili, N. K. Timofeyuk and N. Summers, *Nuclear reactions involving weakly bound nuclei, Experimental Nuclear Physics in Europe, 21-26 June 1999, Seville, Spain*, ed. B. Rubio, M. Lozano and W. Gelletly (AIP Conf Proc. 495 American Institute of Physics, 1999), p. 297.
- 26) D. Bazin et al., *Phys. Rev. Lett.* **74** (1995), 3569.
- 27) P. Roussel-Chomaz, private communication (1996).
- 28) J. S. Al-Khalili, J. A. Tostevin and J. M. Brooke, *Phys. Rev.* **C55** (1997), R1018.
- 29) D. Ridikas, M. H. Smedberg, J. S. Vaagen and M. V. Zhukov, *Europhys. Lett.* **37** (1997), 385.
- 30) G. D. Alkhasov, M. N. Andronenko, A. V. Dobrovosky, P. Egelhof, G. E. Gavrilov, H. Geissel, H. Irnich, A. V. Khazadeev, G. A. Korolev, A. A. Lobodenko, G. Münzenberg, M. Mütterer, S. R. Neumaier, F. Niskel, W. Schwab, D. M. Seliverstov, T. Suzuki, J. P. Theobald, N. A. Timofeev, A. A. Vorobyov and V. I. Yatsoura, *Phys. Rev. Lett.* **78**

- (1997), 2313.
- 31) J. A. Tostevin, J. S. Al-Khalili, M. Zahar, M. Belbot, J. J. Kolata, K. Lamkin, D. J. Morrissey, B. M. Sherrill, M. Lewitowicz and A. H. Wuosmaa, *Phys. Rev.* **C56** (1997), R2929.
  - 32) J. S. Al-Khalili and J. A. Tostevin, *Phys. Rev.* **C57** (1998), 1846.
  - 33) J. A. Tostevin and J. S. Al-Khalili, *Phys. Rev.* **C59** (1999), R5.
  - 34) J. S. Al-Khalili, I. J. Thompson and J. A. Tostevin, *Nucl. Phys.* **A581** (1995), 331.
  - 35) J. A. Tostevin, R. C. Johnson and J. S. Al-Khalili, *Nucl. Phys.* **A630** (1998), 340c.
  - 36) J. A. Tostevin, S. Rugmai and R. C. Johnson, *Phys. Rev.* **C57** (1998), 3225.
  - 37) P. Banerjee, I. J. Thompson and J. A. Tostevin, *Phys. Rev.* **C58** (1998), 1042.
  - 38) P. Banerjee, J. A. Tostevin and I. J. Thompson, *Phys. Rev.* **C57** (1998), 1337.
  - 39) N. K. Timofeyuk and R. C. Johnson, *Phys. Rev.* **C59** (1999), 1545.
  - 40) G. Baur and H. Rebel, *J. of Phys.* **G20** (1994), 1.
  - 41) J. A. Tostevin, S. Rugmai, R. C. Johnson, H. Okamura, S. Ishida, N. Sakamoto, H. Otsu, T. Uesaka, T. Wakasa, H. Sakai, T. Niizeki, H. Toyokawa, Y. Tajima, H. Ohnuma, M. Yosoi, K. Hatanaka and T. Ichihara, *Phys. Lett.* **B424** (1998), 219.
  - 42) S. Fortier, S. Pita, J. S. Winfield, W. N. Catford, N. A. Orr, J. Van de Wiele, Y. Blumenfeld, R. Chapman, S. P. G. Chappell, N. M. Clarke, N. Curtis, M. Freer, S. Gales, K. L. Jones, H. Langevin-Joliot, H. Laurent, I. Lhenry, J. M. Maison, P. Roussel-Chomaz, M. Shawcross, M. Smith, K. Spohr, T. Suomijarvi and A. de Vismes, *Phys. Lett.* **B461** (1999), 22.